This is the Pre-Published Version.
The following publication Z. Jin, K. Pan, L. Fan and T. Ding, "Data-Driven Look-Ahead Unit Commitment Considering Forbidden Zones and Dynamic Ramping Rates," in IEEE Transactions on Industrial Informatics, vol. 15, no. 6, pp. 3267-3276, June 2019 is available at https://doi.org/10.1109/TII.2018.2876316.

Data-Driven Look-Ahead Unit Commitment Considering Forbidden Zones and Dynamic Ramping Rates

Ziliang Jin, Kai Pan, *Member, IEEE,* Lei Fan, *Member, IEEE*, and Tao Ding, *Member, IEEE*,

***Abstract*—Look-ahead unit commitment (LAUC) is recently introduced among Independent System Operators (ISOs) in the U.S. to increase generation capacity by committing more generators after day-ahead unit commitment (UC) when facing various uncertainties in the power system operations. However, as the share of intermittent renewable energy increases significantly in the power generation portfolio, the load continues to fluctuate, and unexpected events and market behaviors happen nowadays, the ISOs are facing new critical challenges to maintain the reliability of power system. To systematically manage these uncertainties and corresponding challenges, new advanced approaches are urgently required to improve current LAUC models and solution methods. Therefore, in this paper, we first propose a new formulation to represent forbidden zones and dynamic ramping rate limits, which help capture the system operation status more accurately and hedge against the uncertainties more effectively, and then correspondingly propose a data-driven risk-averse LAUC model. Our computational experiments show how the size of data influence operational decisions and how the inclusion of forbidden zones and dynamic ramping provides better decisions.**

***Index Terms*—Unit Commitment, Data-Driven, Forbidden Zones, Dynamic Ramping Rates.**

I. Nomenclature

A. Sets

$\mathcal{A}$	Distributional ambiguity set.
$\mathcal{B}$	Set of buses.
$\mathcal{G}$	Set of generators.
$\mathcal{G}_b$	Set of generators at bus b.
$\mathcal{E}$	Set of transmission lines linking two buses.
$\mathcal{R}$	Set of the indices of supporting nodes on R-piece piecewise linear approximation.
$\mathcal{Z}_k$	Set of all zones of generator k.
$\mathcal{F}_k$	Set of forbidden zones of generator k.
$\mathcal{N}_k$	Set of normal zones of generator k.

B. Parameters

T	Number of time intervals for the planning horizon.
SU^k	Start-up cost of generator k.
SD^k	Shut-down cost of generator k.
RU_i^k	Ramp-up rate of generator k in zone i.
RD_i^k	Ramp-down rate of generator k in zone i.
RU_{max}^k	The largest ramp-up rate of generator k among all zones.
RD_{max}^k	The largest ramp-down rate of generator k among all zones.
$\underline{C}^k$	Minimal generation output if generator k is on.
$\overline{C}^k$	Maximal generation output if generator k is on.
$\overline{V}^k$	Start-up/shut-down ramp rate of generator k.
δ	Length of each time interval (e.g., 15 min).
r_t	System reserve factor at time interval t.
$P_{min}^{i,k}$	Minimal generation output of generator k in zone i.
$P_{max}^{i,k}$	Maximal generation output of generator k in zone i.
K_m^b	Line flow distribution factor for transmission line m due to the net injection at bus b.
C_m	Transmission capacity of transmission line m.
α_n^k	The n-th break point in the operation range between the minimum and maximum generation amounts of generator k.
$d_{b,t}$	Load at bus b at time interval t.
$W_t(\xi)$	Generation amount of wind and solar generators at time t corresponding to scenario ξ.

C. Decision Variables

1) First-Stage Decision Variables

u_t^k	1 if generator k starts up at time interval t, and 0 otherwise.
y_t^k	1 if generator k is online at time interval t, and 0 otherwise.
$x_{t,k}^{i_n,i_n}$	1 if there is a transition at time interval t from normal zone i_n to normal zone i_n, and 0 otherwise.
$x_{t,k}^{(i_f,i_f),u}$	1 if there is a transition at time interval t from forbidden zone i_f to forbidden zone i_f ramping up, and 0 otherwise.
$x_{t,k}^{(i_f,i_f),d}$	1 if there is a transition at time interval t from forbidden zone i_f to forbidden zone i_f ramping down, and 0 otherwise.
$x_{t,k}^{i,i+1}$	1 if generator k is in zone $i+1$ at time interval t and in zone i at time interval $t-1$, and 0 otherwise.
$x_{t,k}^{i,i-1}$	1 if generator k is in zone $i-1$ at time interval t and in zone i at time interval $t-1$, and 0 otherwise.

2) Second-Stage Decision Variables

$g_t^k(\xi)$	Generation amount of generator k at time interval t corresponding to scenario ξ.

Ziliang Jin is with the Department of Production Engineering, KTH Royal Institute of Technology, Stockholm, Sweden; email: jzsw1228@gmail.com. Kai Pan is with Hong Kong Polytechnic University, Kowloon, Hong Kong; email: kai.pan@polyu.edu.hk. Lei Fan is with Siemens Industry, Inc., Minnesota, USA; email: lei.fan@ieee.org. Tao Ding is with School of Electrical Engineering, Xi'an Jiaotong University, Xi'an, China; email: tding15@mail.xjtu.edu.cn. The work of K. Pan was partially supported by Hong Kong Polytechnic University under Grant 1-ZE73 and Grant G-YBUD.

$f_t^k(\xi)$ Auxiliary variable representing cost corresponding to scenario ξ.

II. Introduction

As the costs of wind turbines and solar panels decrease, the share of renewable energy is continuously increasing. For instance, more than 30% of the total electricity demand covered by California Independent Operation System (CAISO) is served by the renewable energy resources. Nevertheless, the high penetration of intermittent renewable energy brings new system operation challenges. For example, the duck curve [1], which is famous as new pattern of the demand curve of CAISO, significantly complicates the power system operations. This curve decreases sharply when the sun rises in the daytime but increases dramatically during the sunset time. Such changes increase the difficulty of operating the system to schedule the generation resources and accordingly advanced modeling and solutions approaches are called for. To this end, we aim to improve the reliability and flexibility of the system operations under this new trend from two perspectives: accurate modeling and data-driven solution approach.

To begin with, to tackle the fluctuation of the renewable clean energy such as wind and solar, LAUC runs, with shorter planning horizon than day-ahead UC and each time interval being 15 minutes in general, are introduced among ISOs to help improve the economic dispatch as the new uncertain information is updated [2] and [3]. For example, CAISO has the short term UC which has 18 intervals with each interval being 15 minutes. In Midcontinent ISO (MISO), the LAUC covers three hours in which the first hour has four intervals with each interval being 15 minutes and the last two hours have another four intervals with each being 30 minutes. In order to reflect the generating resources' capability of satisfying the load curve, dynamic ramping rate limits and forbidden zones are needed to be described accurately in the LAUC model.

Currently, most studies ([4], [5] and [6]) focus on the formulation of traditional thermal unit commitment without considering the dynamic ramming rates and forbidden zones. In fact, if these two important features are not captured in the LAUC model, the final solution might be impractical for the system operations (see [7] and [8]). In practice, the power generation ramps continuously, which inevitably engenders the generation within forbidden zones for some very short time intervals. The generator may be scheduled within forbidden zones but has to quickly leave there at the highest possible ramping rate in order to reduce the damage to the mechanical system [8] and [7]. Due to the possible generation within the forbidden zones, dynamic ramping rates become a pivotal role in affecting the corresponding decision. As a consequence, an accurate dynamic ramping limit within the formulation is crucial to ensure the reliability of the system. Thus, in practical applications among ISOs, e.g., MISO and CAISO, ramping rate limits are dynamic according to different generation zones. That means ramping rate is essentially a function of the unit's generation amount [9]. In particular, [9] proposes stepwise and piecewise linear function models to capture the dynamic ramping rates, leading to two mixed-integer linear programming (MILP) models for UC.

These models have limitations in monitoring the transition of ramping rates when the generation ramps across different zones (such as from normal generation zones to forbidden zones). In addition, [10] further improves the models based on [9] by incorporating more realistic cases.

Nevertheless, the model in [10] cannot capture dynamic ramping rate limits when forbidden zones are considered because of the special requirements of forbidden zones [11]. In order to overcome the aforementioned drawbacks of nowadays UC models, we proposed an LAUC model with dynamic ramping rate limits and forbidden zones considered practically. In this paper, we capture the forbidden zones and dynamic ramping rates at the same time by using status transition modeling approach. In particular, we use a transition graph to represent all possible status transitions among normal and forbidden zones and define binary variables corresponding to arcs in the graph to indicate in which status the generator should be. This modeling approach has advantages in terms of formulation tightness and computational performance. As shown in [12], the status-transition-based model leads to network flow formulations which enable commercial mixed-integer linear programming (MILP) solvers such as CPLEX and GUROBI to speed up the solving process.

Next, to better manage the uncertainties due to the penetration of renewable energy, optimization-under-uncertainty techniques are critically important to help improve the decision making. Robust optimization [13] as one of the important tools to hedge uncertainty has been applied in many areas of power system such as unit commitment (e.g., [14] and [15]), self-scheduling generation (e.g., [16]), offering strategy (e.g., [17]), and the planning of plug-in hybrid electric vehicles (e.g., [18]). In particular, for the LAUC model, robust optimization has been applied in MISO and PJM by [19] and [20], respectively, to handle the uncertainties. In addition, stochastic programming has been extensively studied to help make better decision under uncertainty. For instance, [21] and [22] build a two-stage stochastic programming framework for unit commitment problems, [23] and [24] use the two-stage stochastic programming approach to handle the uncertainty in the optimal schedule of micro-grid system. However, robust optimization leads to conservative dispatch results since it considers the worst case [25] and stochastic programming provides a large-sized and computationally difficult model with many possible scenarios, which may generate a suboptimal solution due to limited scenarios. Therefore, in this paper, as indicated in [26] and [27], we propose a data-driven risk-averse two-stage stochastic model to hedge against the uncertainty in the LAUC problem with dynamic ramping rate limits and forbidden zones. In particular, we utilize the historical data of renewable generation outputs to derive a distributional ambiguity set for the uncertain parameters and optimize the total cost against the worst-case distribution in this set, leading to a data-driven risk-averse model. In addition, the risk-averse level can be reduced by increasing more data samples and when the data sample goes to infinity, the data-driven risk-averse model converges to the risk-neutral model. Furthermore, we summarize the differences of our proposed model with traditional approaches as follows:

- Unlike the traditional stochastic programming model, our model does not require a pre-determined distribution of random parameters and can be established and solved directly based on the data.
- Unlike the traditional robust optimization model, the conservativeness of our model can be adjusted based on the number of available data samples, since the confidence set (e.g., $\mathcal{A}_1$ and $\mathcal{A}_\infty$ in the following part) of true distribution is adjustable as the amount of data changes. In particular, the conservativeness of our model goes to zero as the number of available data samples goes to infinity since empirical distribution converges to the true distribution.

The main contributions of our proposed formulation can be summarized as follows:

- We propose an innovative look-ahead unit commitment (LAUC) formulation by simultaneously capturing the dynamic ramping rates and forbidden zones of each generator through the status transition modeling approach. This formulation can readily help improve the reliability and feasibility of system operations.
- We establish a data-driven risk-averse LAUC model with dynamic ramping rate limits and forbidden zones by utilizing the historical available data, leading to more cost-effective and reliable solutions. Meanwhile, the risk-averse level of our proposed model can be simply adjusted based on the amount of available data, which further provides power system operators (e.g., ISOs who are responsible for LAUC runs) an easily implementable solution.
- Extensive computational experiments are performed to show the benefits of considering dynamic ramping rates and forbidden zones and to show the effects of available data on the unit commitment decisions and model conservativeness. In overall, our approach enables a more reliable and stable generation schedule.

We organize the remaining parts of this paper as follows. We first describe the deterministic LAUC model with both dynamic ramping rate limits and forbidden zones in Section III. Then, in Section IV, we derive the data-driven risk-averse two-stage LAUC model by introducing the confidence set construction with L_1 and L_∞ norms, respectively. Furthermore, we develop Benders' decomposition algorithm to solve the corresponding model in Section IV-C. In Section V, we report computational results. Finally, we summarize this paper in Section VI.

III. Deterministic LAUC Model

In this section, we describe the deterministic LAUC problem with dynamic ramping rate limits and forbidden zones as follows:

$$\min \sum_{k\in\mathcal{G}}\sum_{t=1}^{T}\Big(\mathrm{SU}^k u_t^k + \mathrm{SD}^k\left(y_{t-1}^k - y_t^k + u_t^k\right) + F_t^k(\cdot)\Big) \quad (1)$$

$$\text{s.t.} \sum_{i=t-L^k+1}^{t} u_i^k \le y_t^k, \quad \forall t\in[L^k,T], \forall k\in\mathcal{G}, \quad (2)$$

$$\sum_{i=t-\ell^k+1}^{t} u_i^k \le 1 - y_{t-\ell^k}^k, \ \forall t\in[\ell^k,T], \forall k\in\mathcal{G}, \quad (3)$$

$$-y_{t-1}^k + y_t^k - u_t^k \le 0, \quad \forall t\in[1,T], \forall k\in\mathcal{G}, \quad (4)$$

$$x_{t,k}^{i_n,i_n} + x_{t,k}^{i_n-1,i_n} + x_{t,k}^{i_n+1,i_n} = x_{t+1,k}^{i_n,i_n+1} + x_{t+1,k}^{i_n,i_n} + x_{t+1,k}^{i_n,i_n-1}, \ \forall i_n\in\mathcal{N}_k, \forall k\in\mathcal{G}, \quad (5)$$

$$x_{t,k}^{(i_f,i_f),u} + x_{t,k}^{(i_f,i_f),d} + x_{t,k}^{i_f-1,i_f} + x_{t,k}^{i_f+1,i_f} = x_{t+1,k}^{i_f,i_f+1} + x_{t+1,k}^{(i_f,i_f),u} + x_{t+1,k}^{(i_f,i_f),d} + x_{t+1,k}^{i_f,i_f-1}, \quad \forall i_f\in\mathcal{F}_k, \forall k\in\mathcal{G}, \quad (6)$$

$$\sum_{i_n\in\mathcal{N}_k}\left(x_{t,k}^{i_n,i_n} + x_{t,k}^{i_n-1,i_n} + x_{t,k}^{i_n+1,i_n}\right) + \sum_{i_f\in\mathcal{F}_k}\left(x_{t,k}^{(i_f,i_f),u} + x_{t,k}^{(i_f,i_f),d} + x_{t,k}^{i_f-1,i_f} + x_{t,k}^{i_f+1,i_f}\right) = y_t^k, \ \forall t\in[1,T], \forall k\in\mathcal{G}, \quad (7)$$

$$x_{t+1,k}^{(i_f,i_f),u} + x_{t+1,k}^{i_f,i_f+1} \ge x_{t,k}^{i_f-1,i_f} + x_{t,k}^{(i_f,i_f),u}, \quad \forall t\in[1,T], \forall i_f\in\mathcal{F}_k, \forall k\in\mathcal{G}, \quad (8)$$

$$x_{t+1,k}^{(i_f,i_f),d} + x_{t+1,k}^{i_f,i_f-1} \ge x_{t,k}^{i_f+1,i_f} + x_{t,k}^{(i_f,i_f),d}, \quad \forall t\in[1,T], \forall i_f\in\mathcal{F}_k, \forall k\in\mathcal{G}, \quad (9)$$

$$\sum_{k\in\mathcal{G}}\overline{C}^k y_t^k \ge (1+r_t)\sum_{b\in\mathcal{B}} d_{b,t}, \quad \forall t\in[1,T], \quad (10)$$

$$g_{t,j}^k \le \sum_{i\in\mathcal{N}_k}\left(x_{t,k}^{i_n,i_n} + x_{t,k}^{i_n-1,i_n} + x_{t,k}^{i_n+1,i_n}\right)P_{max}^{i_n,k} + \sum_{i\in\mathcal{F}_k}\left(x_{t,k}^{(i_f,i_f),u} + x_{t,k}^{(i_f,i_f),d} + x_{t,k}^{i_f-1,i_f} + x_{t,k}^{i_f+1,i_f}\right)P_{max}^{i_f,k}, \quad \forall t\in[1,T], \forall k\in\mathcal{G}, \quad (11)$$

$$g_{t,j}^k \ge \sum_{i\in\mathcal{N}_k}\left(x_{t,k}^{i_n,i_n} + x_{t,k}^{i_n-1,i_n} + x_{t,k}^{i_n+1,i_n}\right)P_{min}^{i_n,k} + \sum_{i\in\mathcal{F}_k}\left(x_{t,k}^{(i_f,i_f),u} + x_{t,k}^{(i_f,i_f),d} + x_{t,k}^{i_f-1,i_f} + x_{t,k}^{i_f+1,i_f}\right)P_{min}^{i_f,k}, \quad \forall t\in[1,T], \forall k\in\mathcal{G}, \quad (12)$$

$$g_{t+1}^k - g_t^k \le \mathrm{RU}_{i_n}^k\delta x_{t+1,k}^{i_n,i_n} + \max\left\{\mathrm{RU}_{max}^k\delta, \overline{V}^k\right\}\left(1 - x_{t+1,k}^{i_n,i_n}\right), \ \forall i_n\in\mathcal{N}_k, \forall t\in[1,T], \forall k\in\mathcal{G}, \quad (13)$$

$$g_t^k - g_{t+1}^k \le \mathrm{RD}_{i_n}^k\delta x_{t+1,k}^{i_n,i_n} + \max\left\{\mathrm{RD}_{max}^k\delta, \overline{V}^k\right\}\left(1 - x_{t+1,k}^{i_n,i_n}\right), \ \forall i_n\in\mathcal{N}_k, \forall t\in[1,T], \forall k\in\mathcal{G}, \quad (14)$$

$$(g_{t+1}^k - P_{min}^{i+1,k})/\mathrm{RU}_{i+1}^k + (P_{max}^{i,k} - g_t^k)/\mathrm{RU}_i^k \le x_{t+1,k}^{i,i+1}\delta + \max\left\{\mathrm{RU}_{max}^k\delta, \overline{V}^k\right\}/\min\left\{\mathrm{RU}_{i+1}^k, \mathrm{RU}_i^k\right\}\left(1 - x_{t+1,k}^{i,i+1}\right), \quad \forall i\in\mathcal{Z}_k, \ \forall t\in[1,T], \forall k\in\mathcal{G}, \quad (15)$$

$$(g_t^k - P_{min}^{i,k})/\mathrm{RD}_i^k + (P_{max}^{i-1,k} - g_{t+1}^k)/\mathrm{RD}_{i-1}^k \le x_{t+1,k}^{i,i-1}\delta + \max\left\{\mathrm{RD}_{max}^k\delta, \overline{V}^k\right\}/\min\left\{\mathrm{RD}_{i-1}^k, \mathrm{RD}_i^k\right\}\left(1 - x_{t+1,k}^{i,i-1}\right), \quad \forall i\in\mathcal{Z}_k, \forall t\in[1,T], \forall k\in\mathcal{G}, \quad (16)$$

$$\mathrm{RU}_{i_f}^k\delta x_{t+1,k}^{(i_f,i_f),u} - \max\left\{\mathrm{RU}_{max}^k\delta, \overline{V}^k\right\}\left(1 - x_{t+1,k}^{(i_f,i_f),u}\right) \le g_{t+1}^k - g_t^k \le \mathrm{RU}_i^k\delta x_{t+1,k}^{i_f,i_f,u} + \max\left\{\mathrm{RU}_{max}^k\delta, \overline{V}^k\right\}\left(1 - x_{t+1,k}^{(i_f,i_f),u}\right), \ \forall i_f\in\mathcal{F}_k, \forall t\in[1,T], \forall k\in\mathcal{G}, \quad (17)$$

$$\mathrm{RD}_i^k \delta x_{t+1,k}^{i_f,i_f,d} - \max\left\{\mathrm{RD}_{max}^k \delta, \overline{V}^k\right\}\left(1 - x_{t+1,k}^{(i_f,i_f),d}\right) \leq g_t^k - g_{t+1}^k \leq \mathrm{RD}_i^k \delta x_{t+1,k}^{(i_f,i_f),d} + \max\left\{\mathrm{RD}_{max}^k \delta, \overline{V}^k\right\}\left(1 - x_{t+1,k}^{(i_f,i_f),d}\right), \ \forall i_f \in \mathcal{F}_k, \forall t \in [1,T], \forall k \in \mathcal{G}, \quad (18)$$

$$\sum_{k\in\mathcal{G}} g_t^k = \sum_{b\in\mathcal{B}} d_{b,t} - \sum_{b\in\mathcal{B}} W_t^b, \ \forall t \in [1,T], \quad (19)$$

$$-C_m \leq K_m^b \left(\sum_{k\in\mathcal{G}_b} g_t^k - d_b^t\right) \leq C_m, \quad \forall t \in [1,T], \forall m, \forall b, \quad (20)$$

In the above formulation, the objective function (1) includes the start-up/shut-down and the operation costs. More specifically, $\sum_{k\in G}\sum_{t=1}^{T}\left(\mathrm{SU}^k u_t^k + \mathrm{SD}^k\left(y_{t-1}^k - y_t^k + u_t^k\right)\right)$ represents the total start-up and shut-down costs and $\sum_{k\in G}\sum_{t=1}^{T} F_t^k(\cdot)$ represents the operation cost. Note that the generation cost is a quadratic function, i.e., $F_t^k(g_t^k) = a^k(g_t^k)^2 + bg_t^k + cy_t^k$, which can be approximated by a piecewise linear function with R-pieces. For instance, by following the process described in [28], $F_t^k(g_t^k)$ can be replaced by an auxiliary variable f_t^k with following additional constraints:

$$f_t^k \geq (2a^k\alpha_n^k + b^k)g_t^k + (c^k - a^k\alpha_n^k)y_t^k, \quad \forall t, \forall k, \forall n \in [1,R]. \quad (21)$$

Notice that in constraints (21) α_n^k represents the n-th break point in the operation range between the minimum (i.e., $\underline{C}_k$) and maximum (i.e., $\overline{C}_k$) generation amounts of generator k. The feasible region of the deterministic LAUC problem above is described by (2) - (21). Constraints (2) and (3) describe the minimum-up and minimum-down time limits, respectively. Constraints (2) indicate that if generator k starts up at $t-L^k+1$ (i.e., $y_{t-L^k+1}^k = u_{t-L^k+1}^k = 1$), then it has to stay online for at least L^k time periods until t. Constraints (3) indicate that if generator k shuts down at $t-\ell^k+1$ (i.e., $y_{t-\ell^k}^k = 1,\ y_{t-\ell^k+1}^k = 0$), then it has to stay offline for at least ℓ^k time periods until t. Constraints (4) describe the relationship between y and u. They represent that if generator k is online ($y_t^k = 1$) at time period t and offline ($y_{t-1}^k = 0$) at $t-1$, then it means that generator k starts up ($u_t^k = 1$) at t. Constraints (19) enforce the load balance constraints, and transmission constraints (20) denote the capacity limits of each transmission line (m,n) to ensure network security. Note here that failure rate of network components and investment costs are generally not considered in the LAUC model since it runs for a short planning horizon.

For the remaining constraints describing forbidden zones and dynamic ramping rates, we first introduce the transition graph to represent all possible status transitions (represented by arcs) among normal and forbidden zones, as shown in Fig.1. We define a binary variable corresponding to each arc in the graph to indicate whether this arc is active or not. If yes, it indicates that the generator changes the status following that arc. More specifically, given zone i at time t, unit k can have three possible transitions including self-loop arcs (e.g., corresponding to binary variable $x_{t,k}^{i_n,i_n}$), outgoing arcs (e.g., corresponding to binary variables $x_{t,k}^{i,i+1}, x_{t,k}^{i,i-1}$), and incoming arcs (e.g., corresponding to binary variables $x_{t,k}^{i+1,i}, x_{t,k}^{i-1,i}$). Among the arcs in a transition graph, we call one arc an up-transition one if through this transition the generation amount increases and call it a down-transition

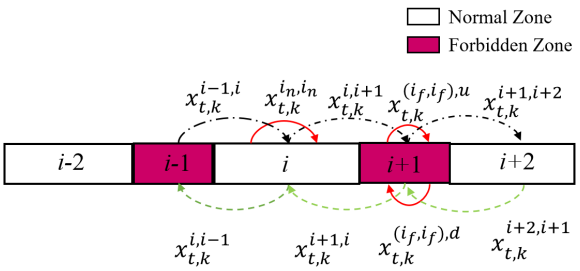

Fig. 1. Transitions Graph

one vice versa. For example, in Fig.1, up-transition arcs (e.g., corresponding to binary variables $x_{t,k}^{i-1,i}$, $x_{t,k}^{i,i+1}$, and $x_{t,k}^{i+1,i+2}$) across two adjoint zones are represented in black dash-dotted lines. Down-transition arcs (e.g., corresponding to binary variables $x_{t,k}^{i,i-1}$, $x_{t,k}^{i+1,i}$, and $x_{t,k}^{i+2,i+1}$) across two adjoint zones are represented in green dashed lines. Note here that a forbidden zone has two self-loop transition arcs, i.e., up-transition and down-transition arcs (e.g., corresponding to binary variables $x_{t,k}^{(i_f,i_f),u}$ and $x_{t,k}^{(i_f,i_f),d}$), respectively. The reason that we distinguish the self-loop up-transition from self-loop down-transition for a forbidden zone is that a forbidden zone is not a stable generation area which requires that the generator must leave the forbidden zone as soon as possible once that generator goes into this forbidden zone.

Therefore, we have constraints (5) (resp. (6)) ensure that if the generator enters normal zone i_n (resp. normal zone i_f) from somewhere at t and then it will definitely stay within normal zone i_n (resp. normal zone i_f) or leave there to somewhere else at $t+1$. Constraints (7) build up the relationships among online/offline status and transition status. That means none of the transitions for generator k will occur once the generator k is offline at time period t ($y_t^k = 0$). Constraints (8) and (9) restrict the operations within forbidden zones. For instance, constraints (8) illustrate an up-transition process that at time t if the generator is ramping up at forbidden zone i_f or just enters this zone i_f from zone $i_f - 1$, then at $t+1$ it has to either keep ramping up at zone i_f or go to zone $i_f + 1$. Correspondingly, a down-transition process is described by constraints (9). Constraints (10) describe the system reserve requirements. Constraints (11) and (12) indicate the generation lower/upper bounds at each time interval, respectively. Constraints (13) - (16) describe the dynamic ramping limits, where (13) and (14) describe the ramping limits in the normal zones and (15) - (16) illustrate the ramping limits across different zones. Constraints (13) enforce the ramping up limits ($\mathrm{RU}_{i_n}^k$) if generator k works in normal zone i_n (i.e., $x_{t+1,k}^{(i_n,i_n),u} = 1$) and otherwise these constraints will be relaxed since $\max\{\mathrm{RU}_{max}^k\delta, \overline{V}^k\}$ is large enough. Constraints (15) represent that if generator k ramps up and crosses over different zones (i.e., $x_{t+1,k}^{i,i+1} = 1$), the ramping rate $\mathrm{RU}^k\delta$ enforced. Otherwise, these constraints will be relaxed too. Similar analysis can be applied to ramping down constraints (14) and (16). Constraints (17) - (18) enforce that once the generator enters the forbidden zone, it has to leave there as quickly as possible and thus its generation ramp-

up/down rates have to take the limits.

IV. Data-Driven Risk-Averse Model

In this section, we propose a data-driven risk-averse two-stage stochastic programming formulation for LAUC Problem (1) with dynamic ramping rates and forbidden zones incorporated and explain how to construct the distributional ambiguity set.

A. Risk-Averse Two-Stage Stochastic Model

In the traditional two-stage stochastic programming framework, the distribution of random parameters is known, e.g., a set of scenarios with each one corresponding to the given probability. In this paper, we assume the net load (i. e., the power load minus renewable generation outputs) is uncertain and thus consider the net load distribution (denoted by P) is unknown and ambiguous. Instead, P can be predefined within a confidence set $\mathcal{A}$ based on the available historical data. The detailed description of the construction of $\mathcal{A}$ is illustrated in Section IV-B. In addition, in our proposed model, we provide optimal decisions on unit commitment and state transitions between different generation zones in the first stage against the worst-case distribution of random parameters in the second stage, where the detailed generation amounts of each generator are decided as recourse. Thus, the corresponding data-driven risk-averse two-stage stochastic LAUC model can be described as follows:

$$\begin{aligned} \min\ & \textstyle\sum_{\forall k,t}\Big(\mathrm{SU}^k u_t^k + \mathrm{SD}^k(y_{t-1}^k - y_t^k + u_t^k)\Big) \\ & + \max_{P\in\mathcal{A}} \mathbb{E}_P[Q(y,u,\xi)] \\ \text{s.t. } & (2)-(10),\ \forall t,k, \end{aligned} \tag{22}$$

where $\mathbb{E}_P[Q(y,u,\xi)]$ represents the expectation under P and $Q(y,u,\xi)$ is equivalent to

$$\begin{aligned} \min\ & \textstyle\sum_{k\in G}\sum_{t=1}^{T} f_t^k(\xi) \\ \text{s.t. } & (11)-(20),\ \text{given } \xi. \end{aligned} \tag{23}$$

Without loss of generality, we use finite possible scenarios, i.e., ξ_1, ξ_2, $\cdots$, ξ_J , with (unknown) probability p_j corresponding to each scenario, respectively, to represent the realization of random parameters and thus the expectation can be represented as follows:

$$\mathbb{E}_P[Q(y,u,\xi)] = \sum_{j=1}^{J} p_j Q(y,u,\xi_j). \tag{24}$$

Note here that, each probability $p_j,\ j=1,\cdots,J$ is random and constrained by the confidence set $\mathcal{A}$.

B. Confidence Set Construction

In this subsection, we introduce the approarch to build the confidence set by following reference [26]. To construct set $\mathcal{A}$ with a given a set of the historical data, we first obtain the empirical distribution through the histogram. In particular, we divide S samples into J bins to fit the historical data. Accordingly, each bin consists of S_1, S_2, $\cdots$, and S_J samples, respectively. In this way, a histogram with $S = \sum_{j=1}^{J} S_j$ is constructed and the empirical distribution for the uncertain electricity demand can be described as $P_0 = (p_1^0, p_2^0, \cdots, p_J^0)^\top$, with $p_1^0 = S_1/S, p_2^0 = S_2/S, \cdots, p_J^0 = S_J/S$. Since the real distribution may be different from the empirical distribution, we define the confidence set for the true distribution by using statistical inference. More specifically, we design two types of confidence sets by using L_1 and L_∞ norms, respectively. When these two norms are used, the empirical distribution can converge to the true distribution as the amount of the historical data (i.e. S) goes to infinity. In addition, another advantage of the utilization of these two norms is that the model can be reformulated as an MILP, which can be solved by commercial solvers. Confidence sets, $\mathcal{A}_1$ and $\mathcal{A}_\infty$ corresponding to L_1 and L_∞ norms, respectively, can be defined as (25) and (26).

$$\begin{aligned} \mathcal{A}_1 &= \{P\in\mathbb{R}_+ | \|P-P_0\|_1 \le \theta\} \\ &= \{P\in\mathbb{R}_+ | \textstyle\sum_{j=1}^{J} |p_j - p_j^0| \le \theta\} \end{aligned} \tag{25}$$

$$\begin{aligned} \text{and } \mathcal{A}_\infty &= \{P\in\mathbb{R}_+ | \|P-P_0\|_\infty \le \theta\} \\ &= \{P\in\mathbb{R}_+ | \max_{1\le j\le J} |p_j - p_j^0| \le \theta\}. \end{aligned} \tag{26}$$

The value of θ in these two norms is defined by the amount of the historical data and the given confidence level. For instance, if the confidence sets are derived by setting the confidence level as 99%, then it means 99% chance is ensured that derived true distribution is within the the given confidence set. Intuitively, the more historical data are used, the closer the distance between the derived empirical distribution and the true distribution is. Therefore, with a fixed confidence level (e.g. 99%), the value θ will decrease if more historical data are available, and as a result of this, the confidence set will shrink. For further description of the relationship between the value θ and historical samples, please refer to the studies in [27] for detailed convergence rates.

C. Benders' Decomposition Algorithm

In this subsection, we reformulate the original model by interchanging the outer summation and inter minimization due to the independence of scenarios ξ_1, ξ_2, $\cdots$, ξ_J, for equation (24). From there, we obtain a max-min problem in the second stage of Problem (22), as shown in the following (27). Furthermore, the inner minization problem can be dualized and integrated with the outer maximization problem, leading to a single maximization problem. Then, Benders' decomposition algorithm can be employed to solve (27) by iteratively solving the mater problem including the first-stage decisions and the sub-problem including the second-stage decisions, where feasibility and optimality cuts are added to the master problem after solving the sub-problem. Since Benders' decomposition framework has been applied for solving many problems in power system operations (e.g., [29], [30], and [31]), we omit the detailed description of Benders' Decomposition algorithm in this paper due to the space limitation.

$$\begin{aligned} \min & \textstyle\sum_{k\in G}\sum_{t=1}^{T}\Big(\mathrm{SU}^k u_t^k + \mathrm{SD}^k(y_{t-1}^k - y_t^k + u_t^k)\Big) \\ & + \max_{P\in\mathcal{A}} \min_g \textstyle\sum_{j=1}^{J} p_j \Big(\sum_{k\in G}\sum_{t=1}^{T} f_t^k(\xi_j)\Big) \end{aligned}$$

$$\text{s.t. } (2)-(10),\ (11)-(20),\ \forall\xi,$$
$$y_t^k,\ x_{t,k}^{(i_n,i_n)},\ x_{t,k}^{(i_f,i_f),u},\ x_{t,k}^{(i_f,i_f),d},\ x_{t,k}^{i,i+1},\ x_{t,k}^{i,i-1} \in \{0,1\},$$
$$f_t^k(\xi)\ free,\ g_t^k(\xi) \geq 0, \forall\xi,\ \forall k,\ t. \tag{27}$$

V. Case Studies

In this section, we perform case studies on various data sets. All the computational experiments (with the optimility gap as 0.01%) are solved by CPLEX 12.7.1 on an Intel-i5 2.3GHz personal computer with 4GB memory. In particular, we first show the effectiveness of our deterministic model with dynamic ramping rates and forbidden zones by comparing it with other existing models in Section V-A. We then extend the experiments to our proposed data-driven model and show how the data impacts the final solutions in Section V-B.

A. Deterministic LAUC

We test our deterministic LAUC model proposed in Section III over the modified IEEE 118-bus system. In particular, we consider six hours in the planning horizon and each time interval corresponds to fifteen minutes, leading to 24 time intervals in total. In addition, we compare four models as follows: 1) "O": our proposed model; 2) "L": the piecewise linear dynamic ramping model presented in [7]; 3) "N": the nominal model without dynamic ramping rates and forbidden zones; 4) "D": the model with forbidden zone presented in [9].

First, the objective costs ($) for Models "O", "L", "N", and "D" are 1130360, 1129820, 1094290, and 1055010 respectively, as "D" achieves the lowest cost since it does not consider ramp rates and "O" has the highest cost since it takes care of more constraints. Next, to prove the effectiveness of our model, we report the generation amounts of Generator 24 over different time periods for illustration in Figure 2. This generator's dynamic ramping rates (MW/min) corresponding to generation ranges (MW) 50 - 70, 70 - 110, 110 - 130, 130 - 167, and 167 - 200 are 1.9, 1.8, 1.7, 1.6, and 1.5, respectively. In addition, the forbidden zones are generation ranges (MW) 70 - 110 and 130 - 167.

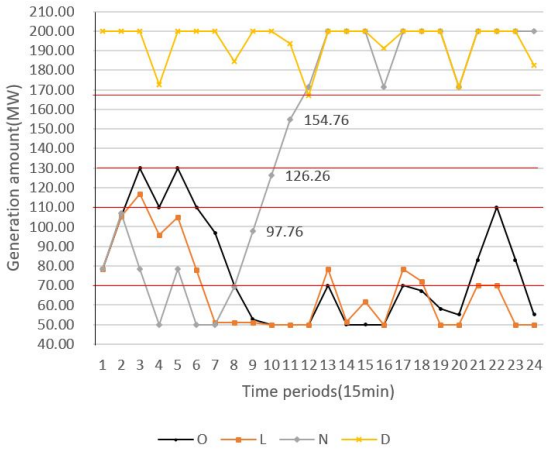

Fig. 2. Dispatch Results of Generator 24 under Different Models

From Figure 2, we can observe that the generator in Model "D" never enters forbidden zones since Model "D" restricts the generation from such zones, while other three models provide possible generation dispatches within forbidden zones. Moreover, between time 9 to time 11, Model "N" keeps ramping up with a fixed ramp rate (i.e., 1.9MW/min), leading to 28.5MW difference between each two time periods. In addition, dispatch results from model "L" show that when the generator enters forbidden zones, generation fluctuates with a low ramping rates (during periods 4 to 6 and 17 to 18), which causes relatively long-time generation in forbidden zones. Technically, it may lead to damages on machines.

In order to better illustrate the advantages of our model, we analyze the generation amounts under different models within the first five time periods, as shown in Table I and Figure 3.

Table I and Figure 3 indicate that the generation amount under Model "O" is in the forbidden zone between time 1 and 2, when it ramps up from 78.5MW to 105.5MW with ramp rate 1.8MW/min. It is the highest possible ramp rate the generator can get in the corresponding forbidden zone. After that, the generator keeps this ramp rate until leaving the forbidden zones and ends up with 130MW at time 3. Model "O" enforces that once the generator enters the forbidden zone, it has to leave there within the least number of intervals. In contrast, during these time periods, Model "N" provides dispatch results where the generator ramps up and down and thus stays in the forbidden zones for longer time with various ramp rates. Similarly, from times 3 to 5, the generation under Model "L" ramps down and up and thus enters and stays in the forbidden zone for a relatively long time.

TABLE I
Generation in the First Five Time Periods

Peirods		1	2	3	4	5
Gen(MW)	O	78.50	105.50	130.00	110.00	130.00
	L	78.50	105.50	116.67	95.65	105.12
	N	78.50	107.00	78.50	50.00	78.50
	D	200.00	200.00	200.00	172.63	200.00

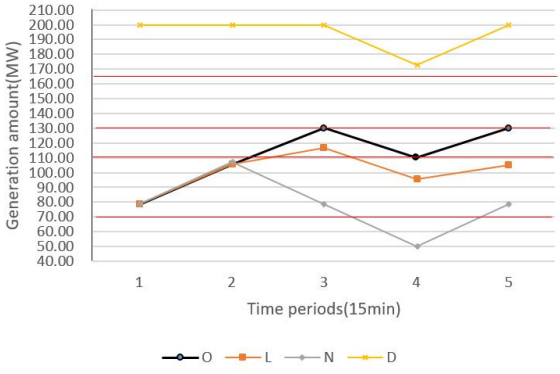

Fig. 3. Generation in First Five Time Periods

Based on the analyses above, it can be verified that our model is able to lead to a more reliable and stable generation operation by better considering the forbidden zones and dynamic ramping rates, as compared with other models, even though the cost from our model is more conservative.

B. Data-Driven LAUC

In this section, we test the proposed data-driven risk-averse two-stage stochastic programming model over the modified IEEE 6-bus and 118-bus systems. We assume the generation from wind farms and solar generator varies and contributes to approximately 15% of the total demand. Thus, for simplicity, we consider the renewable generation as negative demand, leading to more fiercely fluctuated net demand. In addition, we choose 6 hours as the total time length and each time interval has 15 minutes, indicating 24 time intervals here. We compare our two models with risk-neutral stochastic programming and robust optimization model. Those four models are denoted as follows: (1) data-driven two-stage stochastic programming model with L_1 norm (DD-1), (2) data-driven two-stage stochastic programming model with L_∞ norm (DD-Inf), (3) traditional two-stage stochastic programming model (TSP), and (4) robust optimization model (RO).

1) Data Setting: Based on the forecast demand from historical data with given mean and variance, we use Monte Carlo sampling method to generate each individual data and set the number of bins as 5 (i.e., $J = 5$).

2) Effects of Historical Data on Unit Commitment: This experiment aims to test the effects of the historical data on the UC decisions (i.e., online/offline statuses) of the proposed model. In the traditional two-stage stochastic problem, the probability of each scenario is given, leading to risk-neutral decisions. In contrast, the data-driven model provides decisions against the worst-case distribution, leading to risk-averse decisions. In addition, with the amount of samples increases, the risk-averse level of data-driven model decreases, which will have effects on the corresponding decisions of the unit commitment. To further investigate these impacts, we report UC decisions of Generator 3 from 6-bus system and Generator 34 from 118-bus system as shown in Tables II - V.

TABLE II
ONLINE/OFFLINE STATUSES OF GENERATOR 3 FROM 6-BUS SYSTEM UNDER L_1 AND L_∞ NORMS

# of samples \ period	1	2	3	4	5	6
5	1	1	1	1	1	1
50	1	1	1	1	1	1
100	1	1	1	1	1	1
500	1	1	1	1	1	1
1000	0	0	0	0	0	0
2000	0	0	0	0	0	0
5000	0	0	0	0	0	0
Risk-neutral	0	0	0	0	0	0

From Tables II - III, we can observe that given more historical data, the generator keeps online in less time and when the amount of data is large enough, the online/offline statuses will be the same with those obtained from risk-neutral two-stage stochastic model as shown in the last row denoted as Risk-neutral. The reason is that when given few historical data, the risk-averse level is so high that the unit should be online to hedge against the possible uncertainty in the future. Conversely, when given a significant amount of data, operators can make more precise decisions on whether or not it is necessary to start up in advance to prepare for the uncertainty in the future. In other words, the generator can start up for providing energy instead of providing reserve for uncertainty, with given a large amount of historical data. In addition, different from the results in Table II provided by our data-drive model, the robust optimization model always enforces generator 3 to be online at all time periods as shown in Table IV, in order to go against the worst-case data samples. Similar results can be observed from Table V.

TABLE III
ONLINE/OFFLINE STATUSES OF GENERATOR 34 FROM 118-BUS SYSTEM UNDER L_1 AND L_∞ NORMS

# of samples \ period	1	2	3	4	5	6
5	1	1	1	1	1	1
50	1	1	1	1	1	1
100	1	1	1	1	1	1
500	0	0	0	0	0	0
1000	0	0	0	0	0	0
2000	0	0	0	0	0	0
5000	0	0	0	0	0	0
Risk-neutral	0	0	0	0	0	0

TABLE IV
ONLINE/OFFLINE STATUSES OF GENERATOR 3 FROM 6-BUS SYSTEM IN ROBUST OPTIMIZATION MODEL

# of samples \ period	1	2	3	4	5	6
5	1	1	1	1	1	1
50	1	1	1	1	1	1
100	1	1	1	1	1	1
500	1	1	1	1	1	1
1000	1	1	1	1	1	1
2000	1	1	1	1	1	1
5000	1	1	1	1	1	1

3) Effects of Historical Data on Conservativeness: We further investigate the effects of the historical data on the conservativeness of our proposed model. More specifically, we report the changes of the objective value (labelled as "OV" in Table VI) and θ as the amount of historical data increases. We set the confidence level γ as 99% and the number of samples increases from 5 to 5000.

TABLE V
ONLINE/OFFLINE STATUSES OF GENERATOR 34 FROM 118-BUS SYSTEM IN ROBUST OPTIMIZATION MODEL

# of samples \ period	1	2	3	4	5	6
5	1	1	1	1	1	1
50	1	1	1	1	1	1
100	1	1	1	1	1	1
500	1	1	1	1	1	1
1000	1	1	1	1	1	1
2000	1	1	1	1	1	1
5000	1	1	1	1	1	1

TABLE VI
EFFECTS OF HISTORICAL DATA IN 6-BUS SYSTEM

# of samples	DD-1		DD-Inf		TSP	RO
	OV($)	θ	OV($)	θ	OV($)	OV($)
5	44042	3.4539	43855	0.6908	34202	44044
50	43575	0.3454	43313	0.0691	34202	54244
100	42815	0.1727	42598	0.0345	34202	54599
500	41763	0.0345	41324	0.0069	34202	56401
1000	36343	0.0173	36103	0.0035	34202	57402
2000	35586	0.0086	35173	0.0017	34202	57973
5000	34733	0.0035	34665	0.0007	34202	60506

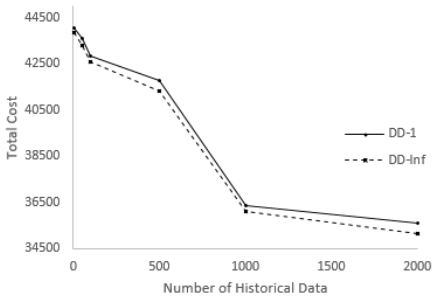

Fig. 4. Effects of Historical Data on the Total Cost in 6-Bus System

TABLE VII
EFFECTS OF HISTORICAL DATA IN 118-BUS SYSTEM

# of sample	DD-1		DD-Inf		TSP	RO
	OV($)	θ	OV($)	θ	OV($)	OV($)
5	1093240	3.4539	1082340	0.6908	947659	1196670
50	1023540	0.3454	1009440	0.0691	947659	1429540
100	999364	0.1727	990601	0.0345	947659	1430068
500	986844	0.0345	980936	0.0069	947659	1710142
1000	967394	0.0173	958087	0.0035	947659	1710661
2000	953374	0.0086	952603	0.0017	947659	1715156
5000	950666	0.0035	949852	0.0007	947659	1815523

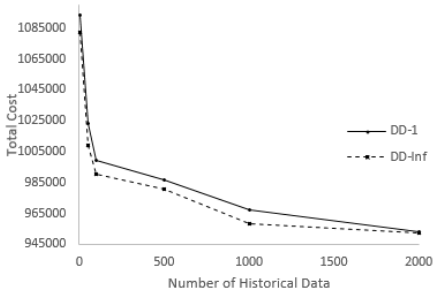

Fig. 5. Effects of Historical Data on the Total Cost in 118-Bus System

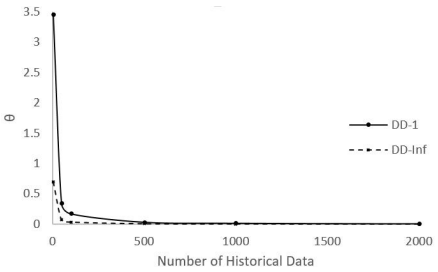

Fig. 6. Effects of Historical Data on the Value of θ in 118-Bus System

From Tables VI - VII and Figures 4 - 6, we can observe that as the amount of historical data increases, both the objective values reported by both data-driven models decrease in both test systems. The reason is that the increase of the amount of historical data leads to a smaller confidence set of the true distribution. Thus, when the amount of historical data is large enough, the data-driven model converges to the risk-neutral stochastic programming model. Furthermore, we find that the robust optimization model always has the highest cost. Furthermore, Figures 4 to 6 show that the convergence rate is fast. As the number of data samples reaches to 1000, the objective values almost converges. In addition, the model DD-1 is more conservative than DD-Inf, because the L_1 norm leads to a larger confidence set compared with L_∞ with the same amount of data samples.

To further understand the value of the extra data samples, we investigate the evolving process of the conservativeness of our models. $Gap_1(s)$ (resp. $Gap_\infty(s)$) is defined to represent the objective value difference between data-driven two-stage stochastic model with L_1 (resp. L_∞) norm and traditional two-stage stochastic model.

$$Gap_1(s) = OBJ_1(s) - OBJ_0, \tag{28}$$

$$Gap_\infty(s) = OBJ_\infty(s) - OBJ_0, \tag{29}$$

where OBJ_0, $OBJ_1(s)$, and $OBJ_\infty(s)$ are the objective values obtained from models TSP, DD-1, and DD-Inf, respectively. Based on the above definitions, we define the value of data as shown in (30) and (31).

$$Vod_1(s,\overline{s}) = \frac{Gap_1(\overline{s}) - Gap_1(s)}{\overline{s} - s},\ for\ \overline{s} > s, \tag{30}$$

$$Vod_\infty(s,\overline{s}) = \frac{Gap_\infty(\overline{s}) - Gap_\infty(s)}{\overline{s} - s},\ for\ \overline{s} > s, \tag{31}$$

TABLE VIII
VALUE OF EXTRA DATA IN 6-BUS SYSTEM

# of sample	DD-1		DD-Inf	
	Gap_1	Vod_1	Gap_∞	Vod_∞
5	9840	N/A	9653	N/A
50	9373	10.38	9111	12.04
100	8613	15.60	8396	14.30
500	7561	2.63	7122	3.19
1000	2141	10.84	1901	10.44
2000	1384	0.76	971	0.93
5000	531	0.28	463	0.17

TABLE IX
VALUE OF EXTRA DATA IN 118-BUS SYSTEM

# of sample	DD-1		DD-Inf	
	Gap_1	Vod_1	Gap_∞	Vod_∞
5	145581	N/A	134681	N/A
50	75881	1548.88	61781	1620.00
100	51705	483.52	42942	376.78
500	39185	31.30	33277	24.16
1000	19735	38.90	10428	45.69
2000	5715	14.02	4944	5.48
5000	3007	0.90	2193	0.91

From Tables VIII and IX, we can observe that both "Gap" and "Vod" decrease as the data sample increases. When the size of the data sample reaches to 2000, the value of the data is

less than 1 for both data-driven models. That means our data-driven model converges to risk-neutral model quickly so that not too much data are needed to obtain relative true solutions.

VI. Conclusions

In this paper, we proposed a data-driven risk-averse two-stage stochastic programming model for the LAUC problem, in which better representations of forbidden zones and of dynamic ramping rates are incorporated. We first presented the deterministic formulation with more accurate physical modeling, with extensive numerical experiments also conducted to verify the advantages of this model as compared to other existing ones. Our model showed that unlike the dispatch from other models, a generator is allowed to dispatch within forbidden zones but has to quickly leave there at the highest possible ramping rate, which proves that our approach enhances the reliability and feasibility of the problem. Next, we provided the corresponding data-driven risk-averse model to hedge against the significant uncertainty in the LAUC runs. Our model utilizes the historical data to construct a distributional confidence set based on the empirical distribution of uncertain parameters, where the true distribution is guaranteed within the set with high confidence level. The impact of the historical data on schedule results was explored and when the data increases to infinity, the decisions converge to those from risk-neutral model. In the future, we would like to explore more physical conditions such as the frequency response capability of the system resource under high penetration of renewable energy resources in the data-driven LAUC model.

References

[1] P. Denholm, M. O'Connell, G. Brinkman, and J. Jorgenson, "Overgeneration from solar energy in california. a field guide to the duck chart," National Renewable Energy Lab.(NREL), Golden, CO (United States), Tech. Rep., 2015.

[2] CAISO, "CAISO Business Practice Manual for Market Operations," https://www.caiso.com/rules/Pages/BusinessPracticeManuals/Default.aspx, 2016.

[3] MISO, "MISO Look-Ahead Tool," https://www.misoenergy.org/WHATWEDO/MARKETENHANCEMENTS/Pages/LookAhead.aspx.

[4] M. Carrión and J. M. Arroyo, "A computationally efficient mixed-integer linear formulation for the thermal unit commitment problem," *IEEE Transactions on Power Systems*, vol. 21, no. 3, pp. 1371–1378, 2006.

[5] J. Ostrowski, M. F. Anjos, and A. Vannelli, "Tight mixed integer linear programming formulations for the unit commitment problem."

[6] K. Pan, Y. Guan, J.-P. Watson, and J. Wang, "Strengthened milp formulation for certain gas turbine unit commitment problems," *IEEE Transactions on Power Systems*, vol. 31, no. 2, pp. 1440–1448, 2016.

[7] T. Ding, R. Bo, W. Gu, and H. Sun, "Big-M based MIQP method for economic dispatch with disjoint prohibited zones," *IEEE Transactions on Power Systems*, vol. 29, no. 2, pp. 976–977, March 2014.

[8] X. Liu, "On compact formulation of constraints induced by disjoint prohibited-zones," *IEEE Transactions on Power Systems*, vol. 25, no. 4, pp. 2004–2005, Nov 2010.

[9] T. Li and M. Shahidehpour, "Dynamic ramping in unit commitment," *IEEE Transactions on Power Systems*, vol. 22, no. 3, pp. 1379–1381, Aug 2007.

[10] C. M. Correa-Posada, G. Morales-España, P. Dueñas, and P. Sànchez-Martìn, "Dynamic ramping model including intraperiod ramp-rate changes in unit commitment," *IEEE Transactions on Sustainable Energy*, vol. 8, no. 1, pp. 43–50, Jan 2017.

[11] CAISO, "Generator Forbidden Operating Regions," https://www.caiso.com/Documents/2360.pdf, 2016.

[12] L. Fan and Y. Guan, "An edge-based formulation for combined-cycle units," *IEEE Transactions on Power Systems*, vol. 31, no. 3, pp. 1809–1819, May 2016.

[13] A. Ben-Tal, L. El Ghaoui, and A. Nemirovski, "Robust optimization. princeton series in applied mathematics," 2009.

[14] R. Jiang, J. Wang, and Y. Guan, "Robust unit commitment with wind power and pumped storage hydro," *IEEE Transactions on Power Systems*, vol. 27, no. 2, p. 800, 2012.

[15] D. Bertsimas, E. Litvinov, X. A. Sun, J. Zhao, and T. Zheng, "Adaptive robust optimization for the security constrained unit commitment problem," *IEEE Transactions on Power Systems*, vol. 28, no. 1, pp. 52–63, 2013.

[16] R. A. Jabr, "Worst-case robust profit in generation self-scheduling," *IEEE Transactions on Power Systems*, vol. 24, no. 1, pp. 492–493, 2009.

[17] L. Baringo and A. J. Conejo, "Offering strategy via robust optimization," *IEEE Transactions on Power Systems*, vol. 26, no. 3, pp. 1418–1425, 2011.

[18] A. H. Hajimiragha, C. A. Canizares, M. W. Fowler, S. Moazeni, A. Elkamel *et al.*, "A robust optimization approach for planning the transition to plug-in hybrid electric vehicles," *IEEE Transactions on Power Systems*, vol. 26, no. 4, pp. 2264–2274, 2011.

[19] Y. Chen, Q. Wang, X. Wang, and Y. Guan, "Applying robust optimization to MISO look-ahead commitment," in *2014 IEEE PES General Meeting Conference*, July 2014, pp. 1–5.

[20] Q. Wang, X. Wang, K. Cheung, Y. Guan, and F. S. S. Bresler, "A two-stage robust optimization for pjm look-ahead unit commitment," in *2013 IEEE PES General Meeting Conference*, June 2013, pp. 1–6.

[21] S. Takriti, J. R. Birge, and E. Long, "A stochastic model for the unit commitment problem," *IEEE Transactions on Power Systems*, vol. 11, no. 3, pp. 1497–1508, Aug 1996.

[22] Q. Wang, Y. Guan, and J. Wang, "A chance-constrained two-stage stochastic program for unit commitment with uncertain wind power output," *IEEE Trans. Power Syst.*, vol. 27, no. 1, pp. 206–215, 2012.

[23] M. Alipour, B. Mohammadi-Ivatloo, and K. Zare, "Stochastic scheduling of renewable and chp-based microgrids," *IEEE Transactions on Industrial Informatics*, vol. 11, no. 5, pp. 1049–1058, 2015.

[24] H. Farzin, M. Fotuhi-Firuzabad, and M. Moeini-Aghtaie, "Stochastic energy management of microgrids during unscheduled islanding period," *IEEE Transactions on Industrial Informatics*, vol. 13, no. 3, pp. 1079–1087, 2017.

[25] C. Zhao and Y. Guan, "Unified stochastic and robust unit commitment," *IEEE Transactions on Power Systems*, vol. 28, no. 3, pp. 3353–3361, 2013.

[26] C. Zhao and Y. Guan, "Data-driven stochastic unit commitment for integrating wind generation," *IEEE Transactions on Power Systems*, vol. 31, no. 4, pp. 2587–2596, July 2016.

[27] K. Pan and Y. Guan, "Data-driven risk-averse stochastic self-scheduling for combined-cycle units," *IEEE Transactions on Industrial Informatics*, vol. PP, no. 99, pp. 1–1, 2017.

[28] R. Jiang, J. Wang, and Y. Guan, "Robust unit commitment with wind power and pumped storage hydro," *IEEE Transactions on Power Systems*, vol. 27, no. 2, pp. 800–810, May 2012.

[29] W. Zhang, Y. Xu, Z. Dong, and K. P. Wong, "Robust security constrained-optimal power flow using multiple microgrids for corrective control of power systems under uncertainty," *IEEE Transactions on Industrial Informatics*, vol. 13, no. 4, pp. 1704–1713, Aug 2017.

[30] R. Deng, G. Xiao, and R. Lu, "Defending against false data injection attacks on power system state estimation," *IEEE Transactions on Industrial Informatics*, vol. 13, no. 1, pp. 198–207, Feb 2017.

[31] J. Soares, B. Canizes, M. A. F. Ghazvini, Z. Vale, and G. K. Venayagamoorthy, "Two-stage stochastic model using benders' decomposition for large-scale energy resource management in smart grids," *IEEE Transactions on Industry Applications*, vol. 53, no. 6, pp. 5905–5914, Nov 2017.

Ziliang Jin received the Bachelor of Management Science degree in industrial engineering from South China University of Technology, Guangzhou, China, in 2018. He was a Research Assistant in the Department of Logistics and Maritime Studies at the Hong Kong Polytechnic University, Hung Hom, Hong Kong, from March 2018 to June 2018. He is currently a master student in the Department of Production Engineering, KTH Royal Institute of Technology, Stockholm, Sweden. His research interests include stochastic integer programming, scheduling optimization and data-driven optimization.

Kai Pan (S'13-M'16) received the B.S. degree in industrial engineering from Zhejiang University, Hangzhou, China, in 2010, and the M.S. and Ph.D. degrees in industrial and systems engineering from the University of Florida, Gainesville, FL, USA, in 2014 and 2016, respectively. He is currently an assistant professor in the Department of Logistics and Maritime Studies at the Hong Kong Polytechnic University, Hung Hom, Hong Kong. His research interests include stochastic integer programming, data-driven optimization, and energy system applications.

Lei Fan (S'13-M'15) received the B.S. degree in electrical engineering from the Hefei University of Technology, Hefei, China, in 2009 and the Ph.D. degree in Industrial and Systems Engineering at the University of Florida, Gainesville, FL, USA. He was an application enigeer in General Electric from 2015 to 2017. Currently, he is a software engieer in Siemens Industry, Inc. His research interests include optimization of power system operations and energy market analysis.

Kai Pan (S'13-M'15) received the B.S.E.E. and M.S.E.E. degrees from SoutheastUniversity, Nanjing, China, in 2009 and 2012, respectively, and the Ph.D.degree from Tsinghua University, Beijing, China, in 2015. During 2013 and2014, he was a Visiting Scholar in the Department of Electrical Engineeringand Computer Science, University of Tennessee, Knoxville, TN, USA. He iscurrently an Associate Professor in the State Key Laboratory of Electrical Insulationand Power Equipment, the School of Electrical Engineering, Xi'anJiaotong University. His current research interests include electricity markets,power system economics and optimizationmethods, and power system planningand reliability evaluation. He has published more than 60 technical papers andauthored by "Springer Theses" recognizing outstanding Ph.D. research aroundtheworld and across the physical sciences—Power System Operationwith LargeScale Stochastic Wind Power Integration. He received the excellent master anddoctoral dissertation from Southeast University and Tsinghua University, respectively,and Outstanding Graduate Award of Beijing City.Dr. Ding is an Associate Editor of CSEE Journal of Power and Energy Systems.